PROCEEDINGS OF SCIENCE

Interpretation of angular distributions of Z-boson production

Jen-Chieh Peng[*]
Department of Physics, University of Illinois at Urbana-Champaign, Urbana, IL 61801, USA
E-mail: jcpeng@illinois.edu

Wen-Chen Chang
Institute of Physics, Academia Sinica, Taipei 11529, Taiwan
E-mail: changwc@phys.sinica.edu.tw

Randall Evan McClellan
Thomas Jefferson National Accelerator Facility, Newport News, VA 23606, USA
E-mail: randallm@jlab.org

Oleg Teryaev
Bogoliubov Laboratory of Theoretical Physics, JINR, 141980 Dubna, Russia
E-mail: teryaev@theor.jinr.ru

We present an intuitive approach for describing the angular distributions of leptons produced in the Drell-Yan process and Z-boson production in hadron-hadron collisions. We show that this approach can describe the pronounced transverse-momentum dependence of the λ and ν parameters, observed at the γ^*/Z production at Tevatron and LHC, very well. The violation of the Lam-Tung relation is attributed to the mis-alignment of the hadronic plane and the quark plane in this approach, and can be well described in this approach.

QCD Evolution 2016
May 30-June 03, 2016
National Institute for Subatomic Physics (Nikhef), Amsterdam

[*]Speaker.

PoS(QCDEV2016)044

1. Introduction

The lepton angular distributions in the Drell-Yan process potentially carry important information on the dynamics of the reaction and on the partonic structures of the colliding hadrons. In the naive Drell-Yan model [1], it was predicted that quark and antiquark annihilat into a transversely polarized photon, leading to a $1+\cos^2\theta$ lepton angular distribution. While this prediction was soon confirmed by the earliest Drell-Yan experiments [2], a more general angular distribution expression is expected when the intrinsic transverse momentum of the partons and/or the QCD effects are included, namely [3],

$$\frac{d\sigma}{d\Omega} \propto 1+\lambda \cos^2\theta + \mu \sin 2\theta \cos\phi + \frac{\nu}{2} \sin^2\theta \cos 2\phi, \tag{1.1}$$

where θ and ϕ refer to the polar and azimuthal angle, of the l^- in the dilepton rest frame. The azimuthal symmetry in the collinear naive Drell-Yan model is lost due to the finite transverse momentum (q_T) of the dilepton. While $\lambda = 1, \mu = \nu = 0$ for the naive Drell-Yan model, the finite value of q_T leads to $\lambda \neq 1$ and $\mu, \nu \neq 0$. Nevertheless, it was pointed out by Lam and Tung that the deviation of λ from 1 is related to the deviation of ν from zero through the relation, $1-\lambda = 2\nu$ [3]. This "Lam-Tung" relation was also predicted to be insenstive to QCD correction [4].

First measurements of the lepton polar and azimuthal angular distributions were carried out by the CERN NA10 [5] and the Fermilab E615 [6] Collaborations. Surprisingly large violations of the Lam-Tung relation were observed, prompting many novel interpretations. In particular, Boer showed that the presence of the Boer-Mulders function, can explain the violation of the Lam-Tung relation [7]. Results from a Drell-Yan experiment [8] using proton beam were also shown to be consistent with this interpretation. Interesting recent developments include the measurements of the lepton angular distribution of Z-boson production in $p-\bar{p}$ collision by the CDF Collaboration at the Tevatron [9] and in $p-p$ collisions by the CMS Collaboration at the Large Hadron Collider [10]. Both the CDF and CMS data show striking q_T dependencies for λ and ν. Moreover, the high-statistics CMS measurement clearly shows that the Lam-Tung relation is violated even at the large transverse momentum region (p_T up to ~ 300 GeV) where effect from the Boer-Mulders function should be negligible.

We present an interpretation for the CMS and CDF results on the q_T dependencies of the angular distribution coefficients λ and ν, as well as the origin for the violation of the Lam-Tung relation. A more detailed discussion can be found in a recent publication [11].

2. Drell-Yan angular distribution

The angular distribution of the leptons is usually expressed in the rest frame of γ^*/Z. In the Collins-Soper (C-S) frame [12], the $\hat{x}$ and $\hat{z}$ axes lie in the hadron plane formed by the colliding hadrons and the $\hat{z}$ axis bisects the momentum vectors of the two hadrons (see Figure 1). Another plane, called the quark plane, is formed by the axis of the collinear q and $\bar{q}$ which combines into the γ^*/Z and the $\hat{z}$ axis. The momentum unit vector of q is defined as $\hat{z}'$, which has polar and azimuthal angles θ_1 and ϕ_1, as shown in Fig. 1. Finally, the back-to-back l^- and l^+, together with the $\hat{z}$ axis, form the lepton plane. The lepton l^- (e^- or μ^-) from the γ^*/Z decay have polar and azimuthal angle in the C-S frame θ and ϕ in the C-S frame, as shown in Fig. 1. For any given values of θ and ϕ, θ_1 and ϕ_1 can vary over a range of values.

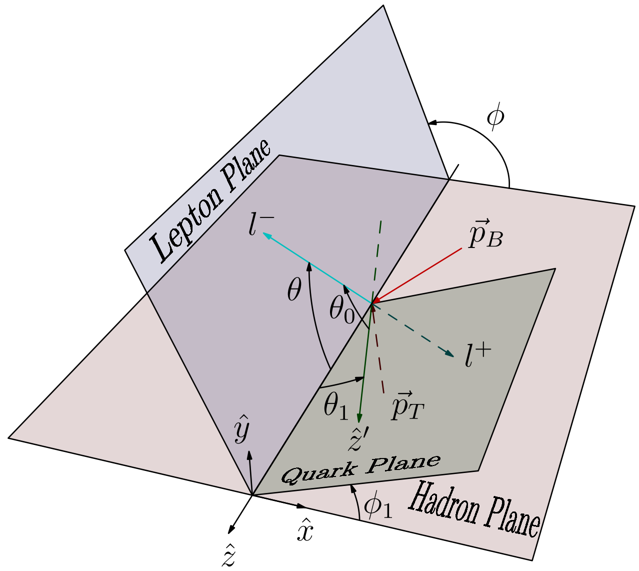

Figure 1: Definition of the Collins-Soper coordinates, the hadron plane, the lepton plane, and the quark plane.

Taking into account the contribution of parity-violating coupling involving the Z boson, the general angular distribution for γ^*/Z production is given as [10]

$$\frac{d\sigma}{d\Omega} \propto (1+\cos^2\theta) + \frac{A_0}{2}(1-3\cos^2\theta) + A_1 \sin 2\theta \cos\phi + \frac{A_2}{2}\sin^2\theta\cos 2\phi + A_3\sin\theta\cos\phi + A_4\cos\theta + A_5\sin^2\theta\sin 2\phi + A_6\sin 2\theta\sin\phi + A_7\sin\theta\sin\phi. \quad (2.1)$$

We show now how this expression can be derived. First, helicity conservation in the $q\bar{q} \to l^- l^+$ reaction implies that the angular distribution of l^- must be azimuthally symmetric with respect to the $\hat{z}'$ axis with the following polar angular dependence:

$$\frac{d\sigma}{d\Omega} \propto 1 + a\cos\theta_0 + \cos^2\theta_0. \quad (2.2)$$

The forward-backward asymmetry coefficient a comes from the parity-violating coupling to the Z boson, and θ_0 is the angle between the l^- momentum vector and $\hat{z}'$, as shown in Fig. 1. To go from Eq. 2.2 to Eq. 2.1, we note that $\cos\theta_0$ satisfies the relation:

$$\cos\theta_0 = \cos\theta\cos\theta_1 + \sin\theta\sin\theta_1\cos(\phi-\phi_1). \quad (2.3)$$

Substituting Eq. 2.3 into Eq. 2.2, we obtain

$$\frac{d\sigma}{d\Omega} \propto (1+\cos^2\theta) + \frac{\sin^2\theta_1}{2}(1-3\cos^2\theta) + (\frac{1}{2}\sin 2\theta_1\cos\phi_1)\sin^2\theta\cos 2\phi + (a\sin\theta_1\cos\phi_1)\sin\theta\cos\phi + (a\cos\theta_1)\cos\theta + (\frac{1}{2}\sin^2\theta_1\sin 2\phi_1)\sin^2\theta\sin 2\phi + (\frac{1}{2}\sin 2\theta_1\sin\phi_1)\sin 2\theta\sin\phi + (a\sin\theta_1\sin\phi_1)\sin\theta\sin\phi. \quad (2.4)$$

From Eq. 2.1 and Eq. 2.4 one can express A_0 to A_7 in terms of θ_1, ϕ_1 and a as follows:

$$\begin{aligned} A_0 &= \langle \sin^2\theta_1 \rangle & A_1 &= \frac{1}{2}\langle \sin 2\theta_1 \cos\phi_1 \rangle \\ A_2 &= \langle \sin^2\theta_1 \cos 2\phi_1 \rangle & A_3 &= \langle a \sin\theta_1 \cos\phi_1 \rangle \\ A_4 &= \langle a \cos\theta_1 \rangle & A_5 &= \frac{1}{2}\langle \sin^2\theta_1 \sin 2\phi_1 \rangle \\ A_6 &= \frac{1}{2}\langle \sin 2\theta_1 \sin\phi_1 \rangle & A_7 &= \langle a \sin\theta_1 \rangle \langle \sin\phi_1 \rangle. \end{aligned} \tag{2.5}$$

Equation 2.5 is a generalization of an earlier work [13] which considered the special case of $\phi_1 = 0$ and $a = 0$. The $\langle \cdot\cdot \rangle$ in Eq. 2.5 is a reminder that the measured values of A_n are averaged over the event sample. A comparison of Eq. 1.1 and Eq. 2.1 gives

$$\lambda = \frac{2-3A_0}{2+A_0}; \quad \mu = \frac{2A_1}{2+A_0}; \quad \nu = \frac{2A_2}{2+A_0}. \tag{2.6}$$

Equation 2.6 shows that the Lam-Tung relation, $1-\lambda = 2\nu$, becomes $A_0 = A_2$.

In the “naive" Drell-Yan the $q-\bar{q}$ axis coincides with the $\hat{z}$ axis of the Collins-Soper frame, hence $\theta_1 = 0$ and $\lambda = 1$. The deviation of λ from the “naive" Drell-Yan prediction of unity is due to non-zero θ_1, which reflects the mis-alignment between the $q-\bar{q}$ axis and the $\hat{z}$ axis of the Collins-Soper frame [13, 14]. It is important to note that λ (or A_0) does not depend on ϕ_1, which is a measure of the non-coplanarity between the $q-\bar{q}$ axis and the hadron plane. In contrast, μ and ν (or A_1 and A_2) depend on both θ_1 and ϕ_1.

Equation 2.6 also shows that the Lam-Tung relation, $A_0 = A_2$, is valid when $\phi_1 = 0$, i.e., for the co-planar case. Violation of the Lam-Tung relation is caused by the presence of the $\langle \cos 2\phi_1 \rangle$ term in A_2 (or ν), and not due to the A_0 (or λ) term. Moreover, the non-coplanarity factor, $\langle \cos 2\phi_1 \rangle$, can be extracted from the data via the ratio A_2/A_0.

In perturbative QCD at the order of α_s, ignoring the intrinsic transverse momenta of the colliding partons, the $q\bar{q} \to \gamma^*/ZG$ annihilation process gives [15, 16, 17]

$$\langle \sin^2\theta_1 \rangle = \sin^2\theta_1 = q_T^2/(Q^2+q_T^2) \tag{2.7}$$

in the Collins-Soper frame, where q_T and Q are the transverse momentum and mass, respectively, of the dilepton. One notes that θ_1 given in Eq. 2.7 is identical to the angle between $\vec{P}_B$ (or $\vec{P}_T$) and the $\hat{z}$ axis in the Collins-Soper frame.

For the $qG \to \gamma^*/Zq$ Compton process, it was shown [5, 18, 19] that $\langle \sin^2\theta_1 \rangle$ is approximately described by

$$\langle \sin^2\theta_1 \rangle = 5q_T^2/(Q^2+5q_T^2), \tag{2.8}$$

Using Eq. 2.6, the above two equations imply

$$\begin{aligned} \lambda &= \frac{2Q^2-q_T^2}{2Q^2+3q_T^2} & \nu &= \frac{2q_T^2}{2Q^2+3q_T^2} & &(q\bar{q}) \\ \lambda &= \frac{2Q^2-5q_T^2}{2Q^2+15q_T^2} & \nu &= \frac{10q_T^2}{2Q^2+15q_T^2} & &(qG). \end{aligned} \tag{2.9}$$

We note that for both processes, $\lambda = 1$ and $\theta_1 = 0$ at $q_T = 0$, while $\lambda \to -1/3$ and $\theta_1 \to 90^\circ$ as $q_T \to \infty$. Moreover, Eq. 2.9 shows that the Lam-Tung relation, $1-\lambda = 2\nu$, is satisfied for both the $q\bar{q}$ and qG processes at order α_s.

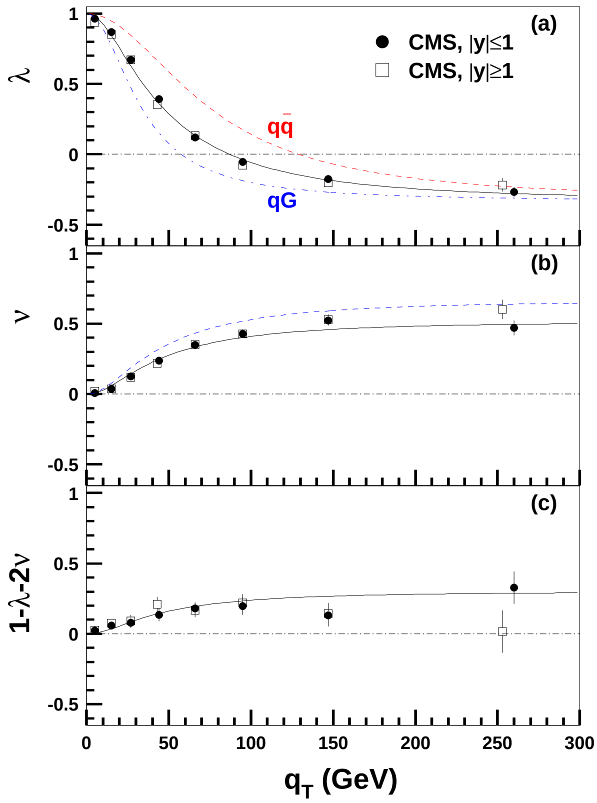

Figure 2: Comparison between the CMS data [10] on γ^*/Z production at two rapidity regions with calculations for (a) λ vs. q_T, (b) ν vs. q_T (c) $1-\lambda-2\nu$ vs. q_T. Curves correspond to calculations described in the text.

3. Comparison with data

The dashed and dash-dotted curves in Fig. 2(a) correspond to the calculation using Eq. 2.9 for the $q\bar{q}$ annihilation and the qG Compton processes, respectively. Both the $q\bar{q}$ and qG processes are expected to contribute to the $pp \to \gamma^*/ZX$ reaction, and the observed q_T dependence of λ must reflect the combined effect of these two contributions. A best-fit to the CMS data is obtained with a mixture of 58.5±1.6% qG and 41.5±1.6% $q\bar{q}$ processes. The solid curve in Fig. 2(a) shows that the data at both rapidity regions can be well described by this mixture of the qG and $q\bar{q}$ processes. In pp collision the qG process is expected to be more important than the $q\bar{q}$ process, in agreement with the best-fit result. While the amount of qG and $q\bar{q}$ mixture can in principle depend on the rapidity, y, the CMS data indicate a very weak, if any, y dependence. The good description of λ shown in Fig. 2(a) also suggests that higher-order QCD processes are relatively unimportant.

We next consider the CMS data on the ν parameter. As shown in Eqs. 2.5 and 2.6, ν depends not only on θ_1, but also on ϕ_1. In leading order α_s where only a single undetected parton is present in the final state, the $q-\bar{q}$ axis must be in the hadron plane, implying $\phi_1 = 0$ and the Lam-Tung relation is satisfied. We first compare the CMS data, shown in Fig. 2(b), with the calculation for ν using Eq. 2.9, which is obtained at the leading order α_s. The dashed curve uses the same mixture of 58.5% qG and 41.5% $q\bar{q}$ components as deduced from the λ data. The data are at a variance with this calculation, suggesting the presence of higher-order QCD processes leading to a non-zero value of ϕ_1. We performed a fit to the ν data allowing a non-zero value of ϕ_1. The best-fit value is $A_2/A_0 = 0.77 \pm 0.02$. The solid curve in Fig. 2(b), corresponding to the best-fit, is in better agreement with the data. The non-zero value of ϕ_1 also implies that the Lam-Tung relation is violated. This violation is indeed observed at CMS and shown explicitly in Fig. 2(c). The solid curve obtained with $A_2/A_0 = 0.77$ describes the observed violation of the Lam-Tung relation well.

The violation of the Lam-Tung relation reflects the non-coplanarity between the $q-\bar{q}$ axis and the hadron plane. This can be caused by higher-order QCD processes, where multiple partons are present in the final state in addition to the detected γ^*/Z. To illustrate this, one considers a specific quark-antiquark annihilation diagram at order α_s^2 in which both the quark and antiquark emit a gluon before they annihilate. The hadron plane in this case is related to the vector sum of the two emitted gluons, and the $q-\bar{q}$ axis is in general not in the hadron plane. This would lead to a non-zero ϕ_1 and a violation of the Lam-Tung relation. Similar consideration would also explain why the intrinsic transverse momenta of the colliding quark and antiquark in the “naive" Drell-Yan could also lead to the violation of the Lam-Tung relation, since the vector sum of the two uncorrelated transverse momenta would lead in general to a non-zero value of ϕ_1.

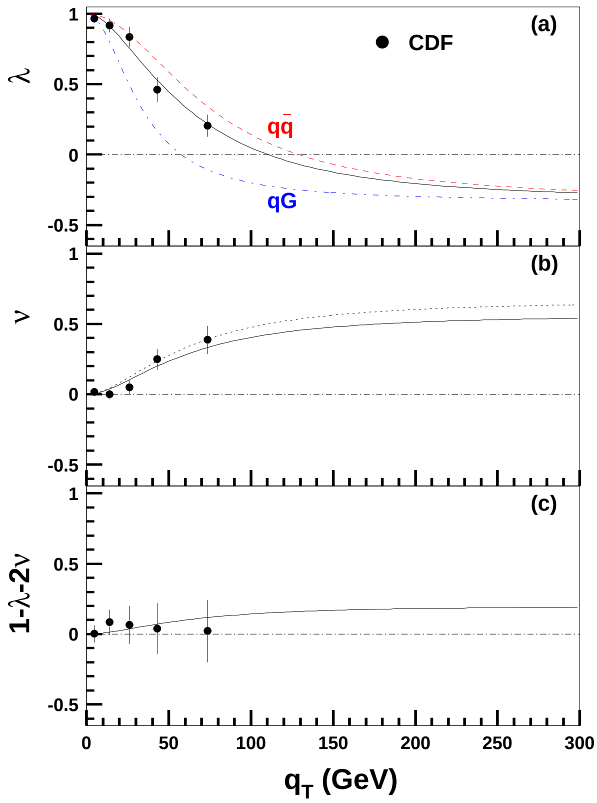

Figure 3: Comparison between the CDF data [9] on γ^*/Z production with calculations for (a) λ vs. q_T, (b) ν vs. q_T (c) $1-\lambda-2\nu$ vs. q_T. Curves correspond to calculations described in the text.

There remains the question why the CDF $\bar{p}p$ Z-production data are consistent with the Lam-

Tung relation [9]. Fig. 3(a) shows λ versus q_T in $\bar{p}p$ collision at 1.96 TeV from CDF. The q_T range covered by the CDF measurment is not as broad as the CMS, and the statistical accuracy is somewhat limited. Nevertheless, a striking q_T dependence of λ is observed. The dashed and dash-dotted curves are calculations using Eq. 2.9 for the $q\bar{q}$ annihilation and the qG Compton processes, respectively. The solid curve in Fig. 3(a) shows that the CDF data can be well described with a mixture of 72.5% $q\bar{q}$ and 27.5% qG processes. This is consistent with the expectation that the $q\bar{q}$ annihilation has the dominant contribution to the $\bar{p}p \to \gamma^*/ZX$ reaction. The CDF data on the ν parameter, shown in Fig. 3(b), are first compared with the calculation (dotted curve) using Eq. 2.9 with a mixture of 72.5% $q\bar{q}$ and 27.5% qG deduced from the λ data. The solid curve in Fig. 3(b) results from a fit allowing A_2/A_0 to deviate from unity. The best-fit value is $A_2/A_0 = 0.85 \pm 0.17$. The relatively large undertainties The quantity $1-\lambda-2\nu$, which is a measure of the violation of Lam-Tung relation, is shown in Fig. 3(c). The solid curve in Fig. 3(c) is obtained using $A_2/A_0 = 0.85$. The CDF data is consistent with the solid curve, and the presence of some violation of the Lam-Tung relation can not be excluded by the CDF data.

4. Conclusion

We have presented an intuitive explanation for the observed q_T dependencies of λ and ν for the CMS and CDF γ^*/Z data. The violation of the Lam-Tung relation can be attributed to the non-coplanarity of the $q-\bar{q}$ axis and the hadron plane, which occur for QCD processes involving at least two gluons. The present analysis could be further extended to the other coefficients, A_1, A_3 and A_4 [20]. It could also be extended [21] to the case of fixed-target Drell-Yan experiments, where the non-coplanarity at low q_T can be caused by the intrinsic transverse momenta of the colliding partons in the initial states [20]. The effects of non-coplanarity on other inequality relations, as discussed in Ref. [22], are also being studied.

References

[1] S.D. Drell and T.M. Yan, Phys. Rev. Lett. **25**, 316 (1970); Ann. Phys. (NY) **66**, 578 (1971).

[2] I. R. Kenyon, Rep. Prog. Phys. **45**, 1261 (1982).

[3] C.S. Lam and W.K. Tung, Phys. Rev. **D18**, 2447 (1978).

[4] C.S. Lam and W.K. Tung, Phys. Rev. **D21**, 2712 (1980).

[5] NA10 Collaboration, S. Falciano *et al.*, Z. Phys. **C31**, 513 (1986); M. Guanziroli *et al.*, Z. Phys. **C37**, 545 (1988).

[6] E615 Collaboration, J.S. Conway *et al.*, Phys. Rev. **D39**, 92 (1989); J.G. Heinrich *et al.*, Phys. Rev. **D44**, 1909 (1991).

[7] D. Boer, Phys. Rev. **D60**, 014012 (1999).

[8] Fermilab E866 Collaboration, L.Y. Zhu *et al.*, Phys. Rev. Lett. **99**, 082301 (2007); Phys. Rev. Lett. **102**, 182001 (2009).

[9] CDF Collaboration, T. Aaltonen *et al.*, Phys. Rev. Lett. **106**, 241801 (2011).

[10] CMS Collaboration, V. Khachatryan *et al.*, Phys. Lett. **B750**, 154 (2015).

[11] J.C. Peng, W.C. Chang, R.E. McClellan, and O.V. Teryaev, Phys. Lett. **B758**, 384 (2016).

[12] J.C. Collins and D.E. Soper, Phys. Rev. **D16**, 2219 (1977).

[13] O.V. Teryaev, Proceedings of XI Advanced Research Workshop on High Energy Spin Physics, Dubna, 2005, pp. 171-175.

[14] P. Faccioli, C. Lourenco, J. Seixas, and H. Wohri, Phys. Rev. **D83**, 056008 (2011).

[15] J.C. Collins, Phys. Rev. Lett. **42**, 291 (1979).

[16] D. Boer and W. Vogelsang, Phys. Rev. D **74**, 014004 (2006).

[17] E.L. Berger, J.W. Qiu, and R.A. Rodriguez-Pedraza, Phys. Lett. B **656**, 74 (2007).

[18] R.L. Thews, Phys. Rev. Lett. **43**, 987 (1979).

[19] J. Lindfors, Phys. Scr. **20**, 19 (1979).

[20] W.C. Chang, R.E. McClellan, J.C. Peng, and O.V. Teryaev, unpublished.

[21] M. Lambertsen and W. Vogelsang, Phys. Rev. **D93**, 114013 (2016).

[22] J.C. Peng, J. Roloff, and O.V. Teryaev, Proceedings of DSPIN 2012.

PoS(QCDEV2016)044